

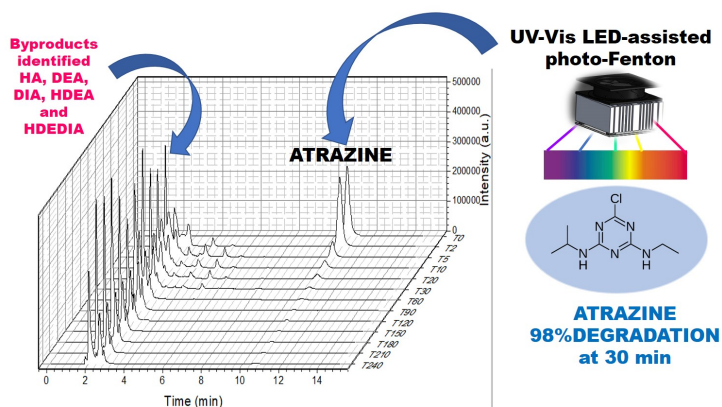
Full Paper | <http://dx.doi.org/10.17807/orbital.v13i2.1531>

Assessment of UV-Vis LED-assisted Photo-Fenton Reactor for Atrazine Degradation in Aqueous Solution

Pedro Luis Sanabria Florez ^{a,b}, Suellen Aparecida Alves ^a, Patricia Los Weinert ^a, and Elaine Regina Lopes Tiburtius* ^a

Atrazine is one of the most used pesticides, although it is extremely toxic for living organisms. In spite of that, the control, removal, and elimination of this agrochemical are still deficient in water treatment plants (just over 25%). For this reason, the main objective of this study was to evaluate atrazine degradation efficiency in aqueous solution using the photo-Fenton system assisted by a light-emitting diode (LED) lamp. The degradation results of 30 mg L⁻¹ atrazine evidenced that our approach presented an efficiency of approximately 98% in only 240 minutes of reaction, and the observed mineralization was 60% of total organic carbon (TOC). Several byproducts were identified (such as HA, DEA, DIA, HDEA, HDIA, and HDEDIA), and the degradation mechanism followed dechlorination and hydroxylation pathways that produce HDEDIA or ammelide. In this way, the photo-Fenton system under an LED lamp showed to be highly efficient at removing atrazine from aqueous solutions, offering several advantages compared to the traditional system, such as lower energy consumption and more environmentally friendly features.

Graphical abstract



Keywords

AOP
Agrotoxic
Atrazine
Led-visible
Photo-fenton

Article history

Received 12 August 2020
Revised 16 June 2021
Accepted 21 June 2021
Available online 25 June 2021

Handling Editor: Sergio R. Lázaro

1. Introduction

Pesticides are among the most widely used organic chemicals in the world due to their importance to food production and agriculture. As a consequence, these compounds are the organic contaminants most frequently found in soil, surface water, and potable water. [1] Atrazine (ATZ; 2-chloro-4-ethylamine-6-isopropylamine-s-triazine) (see

Table S1, Supplementary Material), is a triazine herbicide extensively employed to control weeds in corn, sorghum and sugarcane cultivations. [2] It is especially toxic to the aquatic environment with long-lasting effects [3]. It is classified as one of the most consumed pesticides in the United States, China, and many European countries [4]. In Latin America, it is one of

^a Chemistry Department, State University of Ponta Grossa, Av. General Carlos Cavalcanti, 4748 - CEP 84030-900 Ponta Grossa-PR. ^b Grupo de Investigaciones Ambientales para el Desarrollo Sostenible, Facultad de Química Ambiental, Universidad Santo Tomás, A.A. 1076 Bucaramanga, Colombia. *Corresponding author. E-mail: erltiburtius@uepg.br

the two most used herbicides, and in the Brazilian market of agricultural poisons, ATZ is the third most sold [5].

The widespread and inappropriate use of pesticides has caused adverse environmental impacts on ecosystems and harmful effects on human health. The Environmental Protection Agency (EPA) has classified ATZ as a carcinogenic chemical and an endocrine disruptor [6-10]. Since atrazine presents moderate aqueous solubility, high mobility, and a long half-life (about 250 days) [11], it can be transported by runoff to surface and underground water reservoirs (such as rivers, lakes and subsurface reservoirs), far from the source of contamination [12]. Due to the possible harmful effects of ATZ, some countries, e. g. Germany, the European Union, and some states in the United States such as California, have banned its use [13-15].

Due to the adverse environmental impacts caused by pesticides, a significant amount of research works has been carried out aiming the creation of solutions to eliminate atrazine from water [16]. Conventional methods for water treatment, such as adsorption, sedimentation, and filtration, do not efficiently remove or degrade contaminants such as ATZ [17]. The biologic method is ineffective for ATZ degradation due to the high resistance to biologic degradation [18]. Besides, pesticide solutions are often prepared in water at very high concentrations in the form of emulsions or foams where the pesticides are not dissolved. In this way, the treatment method needs to consider this [19].

Considering the limitations of biological processes and physical-chemical treatments, advanced oxidation processes (AOPs), such as photocatalysis, Fenton [20], photo-Fenton [21] and H_2O_2/O_3 [22] have been proposed as promising alternatives to the conventional water treatments due to their efficiency in the generation of hydroxyl radicals (HO^\bullet). These highly reactive species can oxidize almost all organic compounds and inactivate a wide range of microorganisms. It is reported that the AOPs have been used successfully for the elimination of dyes and pigments, in the treatment of landfill leachate, surface freshwater, potable water and urban wastewater effluents, among others.

Fenton's process is a homogeneous process of catalytic oxidation that uses a mixture of hydrogen peroxide and ferrous ions. [23] In acidic conditions, the addition of hydrogen peroxide to an aqueous medium containing an organic substrate and ferrous ions generates a complex redox reaction. The ferrous ions initiate and catalyze the decomposition of H_2O_2 , which results in the production of hydroxyl radicals, HO^\bullet [24].

In photochemical processes, the light source is a relevant aspect. In recent years, different sources have been reported, such as sunlight and UV radiation, especially with low and medium pressure mercury lamps. The use of these sources has increased the efficiency of photo-Fenton treatments, but their high operational cost associated with high energy consumption, the toxicity of mercury lamps, and low availability of adequate sunlight are major drawbacks [25]. In this scenario, the use of artificial light with low power consumption, long lifespan and ecofriendly nature is required. This need has encouraged the search for new sources of radiation such as light emitting diodes (LEDs), which are more efficient than mercury lamps and not harmful to the environment. Thus, LEDs consist in a promising alternative to mercury lamps and solar radiation to assist photochemical degradation processes. LED semiconductor technology is a directional light source with maximum intensity at a perpendicular angle to the surface emission [26]. Although at

a relatively high cost, LEDs present several advantages compared to traditional lamps since they do not overheat and have a longer useful life, lower energy consumption, and higher luminous efficiency [27]. Also, LEDs exhibit lower light-scattering effects, which is desirable for the treatment of turbid water commonly present in real matrices [28].

In recent years, many authors have investigated the degradation of pollutants such as ATZ through AOPs. Studies have shown the complete degradation of ATZ with mercury lamps and a 99% degradation efficiency using electro-Fenton process. Alternatively, 98% and 94% ATZ degradations have been achieved by using photocatalysis/ozonation [29] and using electrochemical methods [11], respectively. The efficient degradation of ATZ using Fenton and photo-Fenton processes has been extensively reported [31-34]. However, there is a lack of studies towards ATZ degradation that employ UV-Vis LED as the source of radiation, although its use has been reported for the successful elimination of contaminants such as acetamiprid, [35] antipyrine, [36] and diclofenac [37].

The main objective of this study was to evaluate the experimental conditions for the degradation of ATZ (radiation incidence, Fe^{2+} and H_2O_2 concentrations) in a UV-Vis LED-based photo-Fenton approach through a 2^3 full factorial design followed by high-performance liquid chromatography (HPLC) analysis. Furthermore, mineralization was performed as well as the identification of oxidation byproducts by using ultra-performance liquid chromatography tandem mass spectrometry (UPLC/MS).

2. Results and Discussion

2.1 Optimization of the experimental conditions

In this study, an ATZ aqueous solution at a concentration of 30 mg L^{-1} was used to establish comparisons with previous studies [38, 39]. Besides, this concentration corresponds to ATZ maximum solubility in water under the investigated conditions [40]. The degradation efficiency usually depends on various factors, such as the characteristics of the lamp, the concentration of contaminants and the concentration of Fenton's reagents. For this reason, the ATZ degradation efficiency was optimized by using a 2^3 full factorial design. The evaluated variables were the concentration of Fe^{2+} ions (X_1), the concentration of H_2O_2 (X_2), and the use of reflector (X_3) in a photo-Fenton degradation system. With this type of design, it was first possible to calculate the main effects of each factor as well as their interactions.

The experimental response is represented by a linear polynomial model. The experimental matrix and the results are shown in Table 1 and Table S2 ([Supplementary Material](#)). The obtained responses are well adjusted to the linear model with a regression coefficient $R^2 = 0.99757$. From the experimental design, it can be observed that the degradation of ATZ is especially influenced by the concentration of ferrous ions, which presented a positive effect on the ATZ degradation. The second most important factor was the H_2O_2 concentration, which also presented a positive effect on the evaluated response.

The increase in H_2O_2 concentration contributes to an increase in the ATZ degradation rate. However, the interaction terms X_1X_3 ($[Fe^{2+}]$ and reflector) and $X_1X_2X_3$ ($[Fe^{2+}]$, $[H_2O_2]$ and reflector) have negative effects, which means that the effect of the reflector does not have a significant contribution on the ATZ degradation efficiency. As evidenced by the obtained

results, the use of the reflector increased the degradation efficiency by less than 1% (when the reflector was used, the degradation of ATZ just increases from 98.3% to 99.3%). In addition to not greatly enhancing the degradation efficiency, the use of a reflector would increase the cost of the system. Hence, it was decided not to use the reflector in subsequent tests. The Pareto chart in Figure 1 displays the significance of the main and interaction effects.

Table 1. (a) Levels of coded factors for the 2^3 full factorial design. (b) Experimental design matrix and obtained degradation percentages (reaction time: 30 min)

(a)				
Independent variables	Code	Levels		
		-1	1	
[Fe ²⁺] (mg L ⁻¹)	X ₁	10	30	
[H ₂ O ₂] (mg L ⁻¹)	X ₂	100	300	
Reflector (qualitative)	X ₃	Without	With	

(b)				
Assay	Variables			Response
	X ₁	X ₂	X ₃	
1	10	100	Without	69.8±0.01
2	30	100	Without	94.1±0.15
3	10	300	Without	80.4±0.78
4	30	300	Without	98.5±0.59
5	10	100	With	82.9±0.65
6	30	100	With	98.3±0.15
7	10	300	With	92.9±0.11
8	30	300	With	99.3±0.04

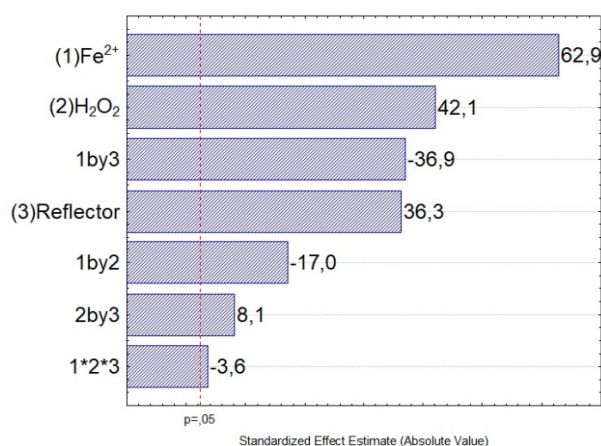


Fig. 1. Pareto chart for the effects resulting from the 2^3 full factorial design employed for the optimization of ATZ (30 mg L⁻¹) degradation through the proposed photo-Fenton approach.

Table 2. ANOVA results for the linear model for ATZ degradation.

Source	Analysis of variance				
	d.f.a	Sum of square	Mean square	F-value	Pr>F
Fe ²⁺	728.1	1	728.1	3951.9	5E ⁻¹²
H ₂ O ₂	326.6	1	326.6	1772.9	1E ⁻¹⁰
Reflector	242.1	1	242.2	1314.6	4E ⁻¹⁰
X ₁ by X ₃	252.0	1	252.1	1368.4	3E ⁻¹⁰
Lack of Fit	2.5	1	2.5	13.3	6E ⁻⁰³
Pure Error	1.5	8	0.2	-	-

Fig. 2 shows that the percent ATZ degradation increases with the concentrations of Fe²⁺ ions and H₂O₂. The removal of ATZ was maximum when the concentrations of Fe²⁺ and H₂O₂ were 30 mg L⁻¹ 300 mg L⁻¹, respectively, and these conditions were employed in all further degradation experiments. The comparison between the actual and the predicted values for ATZ degradation is presented in Fig. 3. There was a great similarity between the actual and predicted values. The statistical significance of the linear model was assessed by analysis of variance (ANOVA), whose results are presented in Table 2. It is frequently reported that increasing the concentration of Fe²⁺ can lead to faster reactions. However, this was not observed in all reactions of this study.

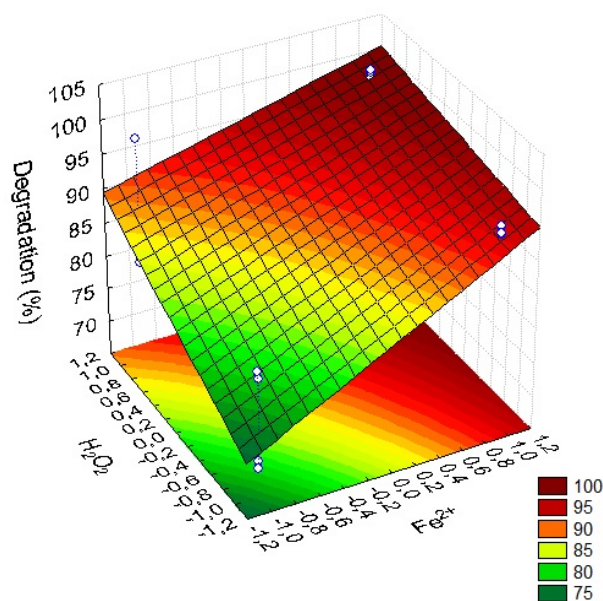


Fig. 2. ATZ degradation percentage as a function of Fe²⁺ and H₂O₂ concentrations.

2.2 ATZ degradation

The kinetics of ATZ removal was investigated up to 240 minutes under optimized conditions for the UV-Vis LED-based photo-Fenton system. Additionally, other processes that could have contributed to the degradation process (H₂O₂/LED and LED-induced photolysis) were assessed (Fig. 4).

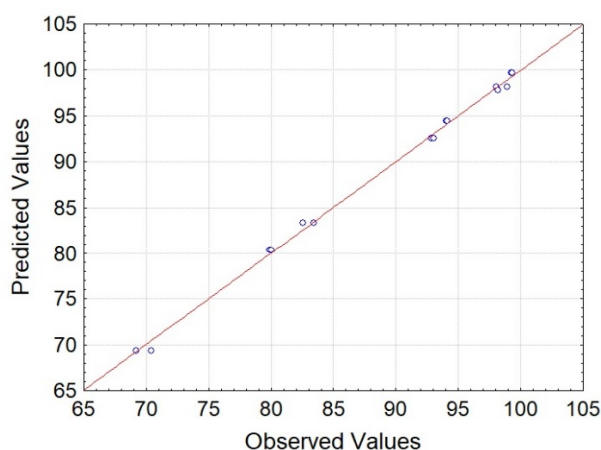


Fig. 3. Comparison of the experimental and predicted values for ATZ degradation.

2.2 ATZ degradation

The kinetics of ATZ removal was investigated up to 240 minutes under optimized conditions for the UV-Vis LED-based photo-Fenton system. Additionally, other processes that could have contributed to the degradation process ($\text{H}_2\text{O}_2/\text{LED}$ and LED-induced photolysis) were assessed (Fig. 4).

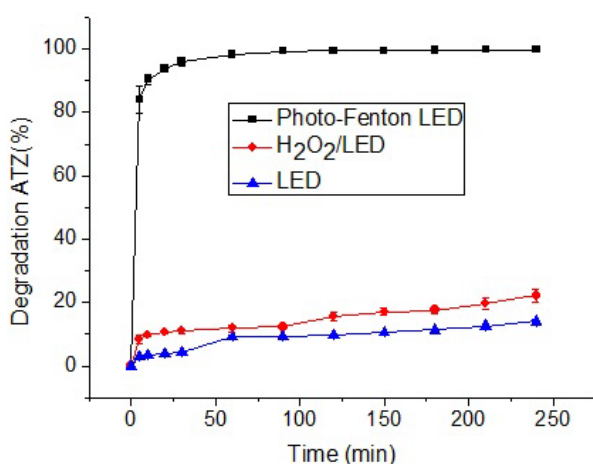


Fig. 4. Degradation profile for UV-Vis LED-based photo-Fenton, $\text{H}_2\text{O}_2/\text{LED}$, and LED-induced photolysis.

Using the UV-Vis LED-based photo-Fenton process, ATZ degradation was almost complete ($> 98\%$), showing high efficiency at 30 min with a degradation of $>80\%$ and these results are comparable with the literature. Several authors have reported different removal processes for ATZ through AOPs. Chan and Chun *et al.*, [21] investigated the degradation of ATZ by using Fenton's reagent as a function of reagent concentrations in a batch reactor. The results demonstrated that the pesticide degradation rates were dependent on the initial concentration of Fe^{2+} e H_2O_2 and were between 15-98%. Acero *et al.* [16] evaluated the degradation kinetics of ATZ (4-5 μM) and identified its degradation products by using O_3 and $\text{O}_3/\text{H}_2\text{O}_2$, reaching efficiencies of 60% after 30 minutes. Lutze *et al.* [64] studied the efficiency of $\text{SO}_4^{\bullet-}$ to degrade ATZ, identified its products and performed a kinetic study. The results showed 70% of ATZ degradation after 35 minutes. Luo *et al.* [56] investigated ATZ degradation by comparing four AOPs, namely UV photolysis, hydrogen peroxide, peroxymonosulfate (HSO_5^-), and persulfate ($\text{S}_2\text{O}_8^{2-}$) using a

low-pressure mercury UV lamp (254 nm). The results showed a 50% efficiency for ATZ removal. Despite these studies, it is difficult to compare results because researchers carry out experiments in different conditions. However, degradation rate achieved in this study ($>98\%$) showed that the UV-Vis LED may substitute mercury lamps with similar efficiency.

To evaluate the effect of direct photolysis and $\text{H}_2\text{O}_2/\text{UV-Vis}$ (280-700 nm) on degradation two experiments were carried out under optimal conditions. In Figure 4, it is possible to observe the effect of these approaches on ATZ degradation. Direct photolysis exhibited a low influence on ATZ degradation, which was approximately 20% at 240 min. The UV radiation source significantly influence the quantum yield for the photodecomposition of ATZ. The quantum yield of decomposition of ATZ by UV irradiation at wavelengths between 200 and 300 nm has been reported to be 0.045 to 0.038 at range concentration from 3 to 33 μM [65]. Indeed, the ATZ percent removal by using $\text{H}_2\text{O}_2/\text{LED}$ was similar to the efficiency obtained in direct photolysis. These results were expected because the photolysis of H_2O_2 occurs at wavelengths lower than 310 nm [66] and the radiation source used in this work ($\lambda = 280$ to 700 nm) does not have enough energy to produce HO^\bullet from H_2O_2 photolysis. This fact showed that the use of Fenton's reagent represents a significant increase in the degradation rate of ATZ.

The kinetic study was performed by using SigmaPlot 12.0 software, and the variation of ATZ concentration as a function of time is presented in Fig. 5. It can be noticed that the degradation process was fast during the first 30 minutes and then slowed down. The velocity law that presented the best fit was related to a two-step pseudo-first-order kinetics with $k_{1\text{obs}} = 0.1445$ and $k_{2\text{obs}} = 0.0476 \text{ min}^{-1}$. These constants are comparable to those reported by Chan and Chu [21] and Kassinos *et al.* [40]. However, k_{obs} values are greater than most of the kinetic coefficients found in the literature for degradation of ATZ. From k_{obs} , the half-life of ATZ was found to be approximately 8.6 min (Table S3).

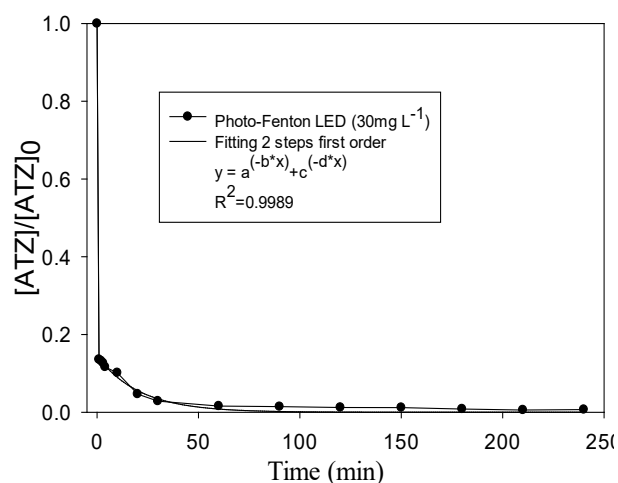


Fig. 5. Kinetic profile for degradation of ATZ employing the proposed UV-Vis LED-based photo-Fenton approach.

2.3 Mineralization of atrazine

The Total Organic Carbon (TOC) content of the initial ATZ solution (30 mg L^{-1}) was determined as 13.22 mg L^{-1} , which is very similar to the theoretical value of 13.33 mg L^{-1} . The TOC content after ATZ removal using the UV-Vis LED-based photo-Fenton for 240 min was found to be 7.93 mg L^{-1} (Fig. 6), which corresponds to 60% of the initially measured TOC. Thus, it can

be inferred that 4.74 out of 8 carbon atoms remained in the solution, that is, only 3 carbon atoms from the ATZ side chains were completely mineralized.

The mineralization of 40% for the ATZ aqueous solution is an important result since it consists in a high rate of mineralization in comparison to the literature for AOPs. For instance, a 40% mineralization efficiency was reached for a TiO₂/O₃ system [41, 42], whereas the photo-Fenton reaction presented a mineralization of 60% [43]. The Fenton reaction has also been used for the degradation of ATZ, whose levels reached 50% [44]. Alternatively, Malpass *et al.* [45] performed the degradation of ATZ (20 mg L⁻¹) via an electrochemical process and obtained 46% TOC removal [45]. McMurray *et al.* [46] studied the photocatalytic degradation of ATZ (20 mg L⁻¹) and obtained 40% TOC removal [46].

Despite the time of treatment, there is still a 60% organic carbon content, which is typical for organic compounds with a short carbon chain. Besides, 80% hydrogen peroxide was consumed after 20 minutes, and this probably affected the mineralization. However, Fe²⁺ concentration has been described as a relevant factor, and it was previously evidenced that sequential Fe²⁺ addition over the reaction time can improve mineralization and give promising results. [31, 47, 48] Regarding the mineralization of ATZ, it was found that a kinetic expression with two first-order steps fit well with the experimental data (R² > 0.99) (Fig. 6). This corresponds to a fast degradation step during the first minutes of reaction, followed by a much slower one.

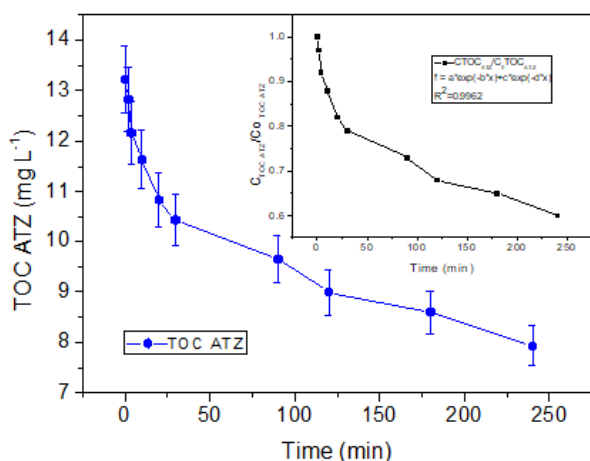


Fig. 6. Degradation of TOC for ATZ and corresponding kinetic profile.

The development and use of LEDs as an alternative source of radiation to mercury lamps have proven to be effective for the degradation and mineralization of various organic pollutants [28]. In spite of that, an even higher effectiveness could be achieved if improvements in radiant efficiency and output power were considered. This would increase the energy efficiency of LEDs, making this technology cost-effective comparing to traditional systems.

2.4 LEDs as a source of radiation in advanced oxidation processes.

The advantages of LEDs over conventional mercury lamps are the absence of filling gas and mercury, no heating and quick start time, small size (which facilitates the design of reactors), much longer life (3,000 h at 250 nm; 26,000 h at 365 nm), monochromatic emission in a range of wavelengths

for a specific performance (210-400 nm) and low voltage requirements of 6–30 V [49]. This allows LEDs to be powered by batteries or solar cells, which enables the construction of portable devices. Small chip sizes provide flexible variability for the LED matrix design (line, plane, surface, three-dimensional models), which produces two conceptual reactor designs with enclosed or covered LED arrays [50]. The development of advanced LED-based oxidation technologies for water treatment requires the selection of a LED with a suitable emission wavelength, long service life, and passive cooling (for high power LEDs). The preferable emission wavelength should be as wide as possible (UVA, NUV, or even visible range) due to considerably higher wall plug efficiency (WPE) values and lower costs for LED with longer wavelengths. Chen *et al.* published a detailed review on the fundamentals, types, performance, matrix and reactor designs for UV-Vis LEDs. Considering these important requirements, we will focus on the efficiency of degradation using LEDs and energy consumption as key parameters for the use of such radiation sources in AOPs [49].

2.4.1 Energy considerations

According to the International Union of Pure and Applied Chemistry (IUPAC), energy consumption is an essential parameter for the evaluation of the efficiency and viability of a water treatment technology. Therefore, the obtained ATZ degradation data were analyzed in terms of electric power consumption (E_{EO}) to determine the energy cost related to the proposed UV-Vis LED-based degradation system. The electrical energy per order E_{EO} (kWh m⁻³) is defined as the number of kilowatt-hours (kWh) of electrical energy required to reduce the concentration of a pollutant and is calculated by using the following equation [51]:

$$E_{EO} = \frac{P \cdot t \cdot 1000}{V \cdot 60 \cdot \log \left(\frac{C_i}{C_f} \right)} \quad (1)$$

where P is the power input (kW) of the wall to derive the lamp; t is the irradiation time (h); V is the volume (L) of the solution in the reactor; C_i and C_f are the initial and final contaminant concentrations, respectively.

Through the use of equation 1, the E_{EO} value for the degradation of 30 mg L⁻¹ ATZ with the UV-Vis LED-based photo-Fenton approach was calculated to be equal to 6.17 kWh m⁻³, which is significantly lower than the values reported in the literature for photo Fenton degradation of this pesticide (Table 3). The E_{EO} value obtained for the developed degradation strategy evidences the outstanding efficiency of the photo Fenton method for the treatment of water contaminated with ATZ, since the values of E_{EO} required to remove this pesticide from industrial wastewater through AOP at a reasonable cost should be between 2.5–5 kWh m⁻³ [52, 53].

2.5 Degradation intermediates

Byproducts derived from the degradation of pesticides may have lower toxicity to the ecosystem compared to their main chemicals [38, 28]. However, in some cases, they may present greater risks to the environment. Therefore, it is extremely important to identify the intermediaries generated in the degradation process. It has been reported that byproducts from ATZ contain s-triazine rings that are resistant to further degradation [40]. Figure 7 shows the

chromatograms obtained during ATZ degradation. The retention time (t_R) of 10.7 minutes corresponds to the studied pesticide. It is clear that this peak decreased fast in the first minutes and completely disappeared at 240 min. However, the degradation of ATZ resulted in the formation of intermediate species since additional peaks could be observed in the chromatograms. After 5 minutes of irradiation, peaks ascribed to the presence of intermediates were observed at $t_R = 2$ to 8 minutes, which gradually decreased until 240 minutes of reaction.

Table 3. Electricity consumption in different reactors reported in the literature for the treatment of water contaminated with ATZ.

Type of AOP	Treatment time (min)	Treated volume (L)	Removal of ATZ (%) [*]	E _{EO} (kWh m ⁻³)	Reference
Anodic oxidation (AO - H ₂ O ₂)	300	1.5	45	76.0	
Electro-Fenton (EF)	300	1.5	61	60.8	[56]
Photoelectro-Fenton (PEF).	300	1.5	99	30.4	
AOP with plasma-assisted	30	2.5	60	33.2	[57]

^{*}ATZ removal after 90 min

After 240 minutes of irradiation, peaks could still be observed between 2 and 3 minutes, which are also related to intermediates generated from ATZ degradation.

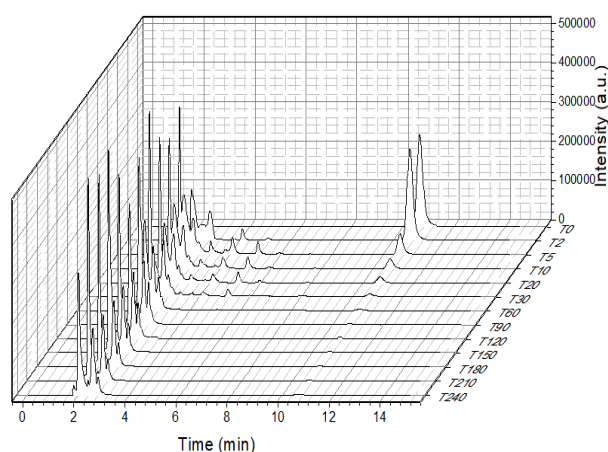


Fig. 7. Chromatograms of ATZ degradation under optimized conditions up to 240 min.

To identify the intermediates resulting from ATZ degradation, the UPLC/MS conditions were optimized to obtain a good resolution, a stronger herbicide signal, and shorter analysis times. Under selected condition, all analytes could be separated, and an appropriate resolution was obtained between the peaks of 2-hydroxy-atrazine (HA), diisopropyl atrazine (DIA), desethylatrazine (DEA), atrazine-desethyl-2-hydroxy (HDEA), atrazine-desisopropyl-2-hydroxy (HDIA) and atrazine-desethyl-desisopropyl-2-hydroxy (HDEDIA or Ammelide). Their primary ions were observed at $[M+H]^+$, $m/z = 216$ for ATZ, $m/z = 198$ for HA, $m/z = 188$ for

DEA, $m/z = 174$ for DIA, $m/z = 170$ for HDEA, $m/z = 156$ for HDIA and $m/z = 128$ for HDEDIA (Fig. S1, Supporting information). The generation of these byproducts must be avoided because triazole derivatives exhibit a wide range of embryotoxic effects. For instance, it has been found that the exposure to triazole can induce skeletal defects, craniofacial malformations and hydrocephalus in rats, including cases of teratogenicity [54, 55].

Two mechanisms for ATZ degradation have been described in the literature [56]: (1) dechlorination-hydroxylation followed by dealkylation and subsequent deamination, and (2) dealkylation as a first step and then deamination and/or dechlorination-hydroxylation. The first mechanism has been reported more frequently, with 2-hydroxytriazine and compounds as major hydroxylated intermediates. According to the results of UPLC/MS from the present study, it is evident that the main byproducts of ATZ degradation with the UV-Vis LED lamp were DIA and DEA. With this piece of information in mind, a route for ATZ degradation can be proposed (Fig. 8). Firstly, oxidation of the side chains takes place to form dealkylated species such as DIA and DEA. Next, dichlorination and hydroxylation reactions yield species such as HDEA and HDIA. Finally, the replacement of the amino groups by hydroxyl molecules takes place, resulting in the species HDEDIA or ammelide, followed by a further deamination step to give cyanuric acid (intermediate not identified).

The obtained results could be attributed to the chemical hydrolysis of ATZ that produces hydroxyatrazine in highly acidic or basic solutions. Alkaline hydrolysis likely involves a direct nucleophilic displacement of Cl⁻ from the two positions of atrazine by OH⁻, while acid hydrolysis may be a result of protonation of a ring or chain nitrogen atom followed by C-Cl bond cleavage by water. That may be the cause of faster hydrolysis of ATZ in alkaline medium compared to acidic medium [57].

3. Material and Methods

3.1 Reagents

ATZ (99.1%) was purchased from Sigma Aldrich (USA). Hydrogen peroxide (50% v/v) and hydrochloric acid were acquired from Neon (Brazil). Acetonitrile (HPLC grade), iron sulfate heptahydrate (Fe(SO₄)₇H₂O) and potassium bisulfite (KHSO₃) were purchased from Merck, Vetec and Biotec, respectively.

3.2 Instrumental methods

For the identification and quantification of ATZ, it was used the method previously described by Jacomini *et al.* [58], with modifications. A high-performance liquid chromatograph equipped with a diode array (DAD) UV detector (Shimadzu-Prominence) was employed as C18 column (particle size of 4.6 μm and 150 mm) was used as a stationary phase. The mobile phase was HPLC grade acetonitrile and ultrapure water in a 40:60 (v/v) ratio, with a flow rate of 0.8 mL min⁻¹. Analyses were performed under isocratic conditions with an injection volume of 20 μL, a column temperature of 40 °C and at the wavelength of 222 nm, allowing short chromatographic series with retention times of 10.7 min (ATZ). The analytical curves for a concentration range between 1.0 and 30 mg L⁻¹ showed R² values of 0.9987 in different days of work. The limit of detection and the limit of quantification were found to be 0.4 mg L⁻¹ and 1.3 mg L⁻¹ respectively.

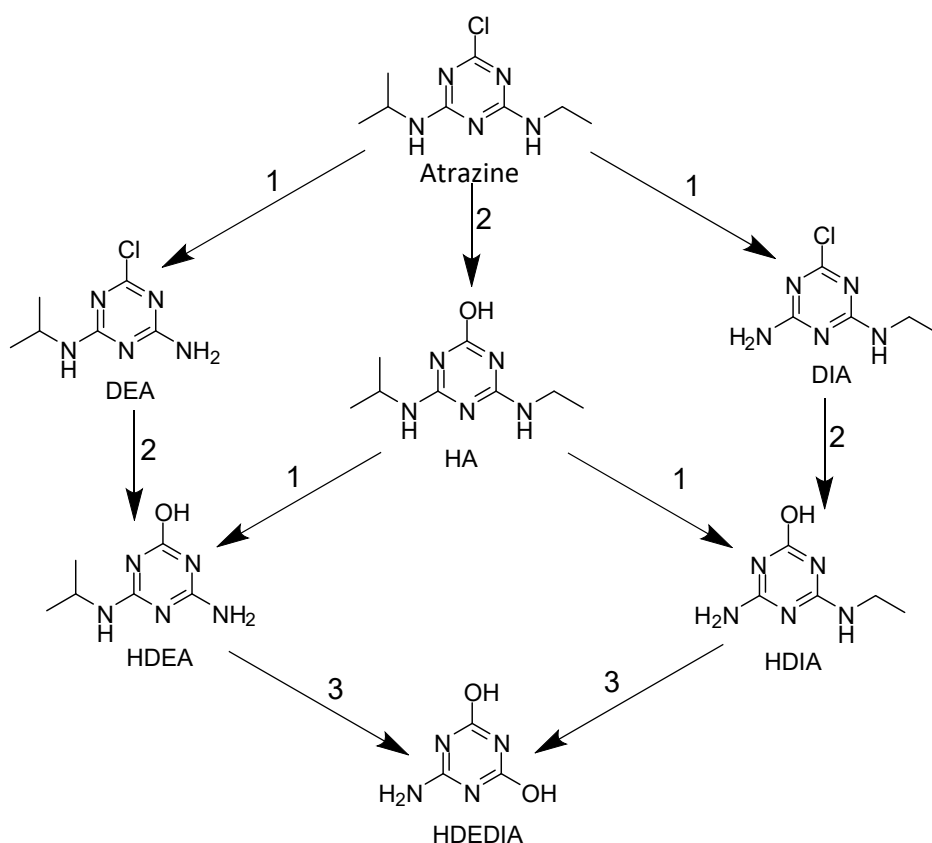


Fig. 8. The proposed possible degradation mechanism via the photo-Fenton LED system. Desalkylation (1), dechlorination-hydroxylation (2) and deamination-hydroxylation (3).

Oxidation products were identified using a UPLC/MS (Acquity and Xevo TQD - Waters chromatograph with an electrospray ionization source (ESI)). A C18 reverse phase column (Agilent; 2.1 mm- 50 mm, 1.7 mm particle size) was used for separation. A 5 μL sample aliquot was injected with an ammonium acetate/acetonitrile eluent at a flow rate of 0.1 $\mu\text{L min}^{-1}$. A TQD Xevo precision mass was used under positive ESI in full scan mode. The operating parameters of ESI were: spray voltage = 1.2 kV, capillary temperature = 350°C, decay potential = 5 V, collision energy = 50 V and exploration range (m/z) = 100 to 810 a.m.u. Before use, the mass spectrometer was calibrated using the tuning solutions recommended by the manufacturer. To find the appropriate conditions for the separation of the studied compounds, C18 column was used and several mobile phases were evaluated. The final results showed that the best mobile phase was composed of acetonitrile:water using a gradient mode as follows: 0-6 min a ratio of 97% H_2O :3% ACN; 6-8 min the proportion of 0% H_2O :100% ACN; and 8-8.1 min of 0% H_2O : 100% ACN at 97% H_2O :3% ACN, which provided the determination of 2-hydroxyatrazine (HA), Desisopropyl atrazine (DIA), Desethylatrazine (DEA), Atrazine-desethyl-2-hydroxy (HDEA), atrazine-desisopropyl-2-hydroxy (HDIA), Atrazine-desethyl-desisopropyl-2-hydroxy (HDEDIA or Ammelide) and ATZ.

Two colorimetric methods were used to determine Fe^{2+} and H_2O_2 concentrations [59] with a UV-Vis Cary 50 spectrophotometer (Varian). TOC-L Shimadzu analyzer was used to monitor Total Organic Carbon (TOC). An analytical curve was obtained with aqueous standards of potassium hydrogen phthalate in the range between 5 and 200 mg L^{-1} . Under these conditions, a typical 2% RSD was observed with $R^2=0.990$ [60].

3.3 ATZ degradation assays

The ATZ degradation was performed using a 30 mg L^{-1} aqueous solution of the pesticide at pH 3 in order to avoid the precipitation of iron hydroxides. The experiments were carried out at room temperature (25 °C) in a cylindrical borosilicate reactor (Fig. 9) with length of 8 cm and capacity of 250 mL. A LED lamp was positioned 3 cm above the reactor. The light emitted by the LED lamp was in the 280-700 nm range (Fig. S2, Supporting information), with a power output of 50 W and 4500 Lumen. The photon flux rate estimate of the lamp toward the solution was measured according to the literature [61-63] by using a ferrioxalate actinometer and was determined to be equal to 2.3×10^{-6} Einstein min^{-1} .

Chromatographic experiments were performed by collecting 2 mL samples of the irradiated solution after each radiation interval, followed by mixing with 0.2 mL of potassium bisulfite to stop the reaction and HPLC analysis to determine ATZ concentration. Each experiment was performed in triplicate; the error bars in the figures represent the standard error of the mean. TOC measurements were conducted in triplicate for each point with 35 mL of the samples. Samples were analyzed immediately after irradiation and 3.5 mL of potassium bisulfite (28%, m/v) were used to quench residual hydrogen peroxide and stop the degradation reaction.

3.4 Experimental design

To evaluate the effect of different parameters in the photo-Fenton LED treatment, a 2^3 full factorial design was carried out. The studied variables were H_2O_2 concentration (mg L^{-1} , X_1), Fe^{2+} concentration (mg L^{-1} , X_2) and use of reflector (X_3). A

total of 16 randomized photo-Fenton-LED degradation experiments were performed. The levels considered for the experimental design are listed in Table 1a. Each assay was performed in triplicate, and the evaluated response was the ATZ concentration determined in duplicate by using HPLC. The coefficients of the polynomial model were calculated by using Statistica 13.0 software.

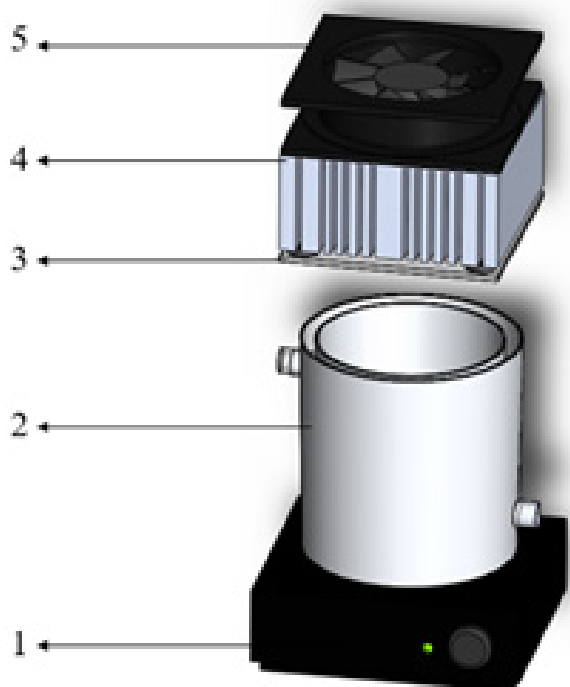


Fig. 9. Schematic diagram of the LED reactor (1: magnetic stirrer, 2: glass reactor, 3: quartz plate, 4: LED lamp, 5: cooling fountain).

4. Conclusions

In this study, the efficiency of a photo-Fenton process in acid medium was demonstrated, using UV-Vis LED as the energy source to eliminate ATZ (30 mg L^{-1}) and its byproducts from aqueous solutions. The UV-Vis LED lamp increased the generation of strongly oxidant HO^\cdot radicals that efficiently degraded ATZ under optimum operating conditions ($[\text{H}_2\text{O}_2] = 300 \text{ mg L}^{-1}$, $[\text{Fe}^{2+}] = 30 \text{ mg L}^{-1}$). Mineralization was measured by employing TOC analysis, and the removal of organic carbon reached 40% at 240 minutes. Furthermore, the degradation by-products were detected by using UPLC/MS, and the results evidenced that the mechanism of ATZ degradation followed firstly dichlorination and hydroxylation steps to form species such as HDEA, and then the replacement of the amino groups by hydroxyl moieties, which results in HDEDIA or ammelide molecules.

The proposed UV-Vis LED-based photo-Fenton degradation system is a potential alternative to degrade pollutants such as atrazine in wastewater. One of the main advantages of the system was the high degradation efficiency and mineralization as a result of the usage of UV-Vis LED as energy source. Furthermore, the presented approach showed to be cost-effective and ecofriendly, which enhances their potential of application in wastewater treatment.

Supporting Information

Table S1. Physical-chemical properties and ATZ chemical structure.

Table S2. Matrix of the 2^3 full experimental design with degradation percentage values (reaction time: 30min).

Fig. S1. UPLC/MS chromatogram of ATZ for the identification of degradation intermediates.

Fig. S2. Emission spectrum of the LED lamp.

Table S3. Kinetic data of degradation of ATZ by using the proposed UV-Vis LED-based photo-Fenton approach (reaction time: 240min).

Acknowledgments

The authors are thankful to CAPES (Commission for the Improvement of Higher Education Personnel in Brazil) and C-LABMU (Complex of Multiuser Laboratories in the State University of Ponta Grossa). We also thank the electronic engineer Raul Osmar Tiburtius for designing and constructing the LED lamp used in the presented assays.

Author Contributions

All authors contributed to the study conception and design. The conduct of research and investigation was performed by Pedro Sanabria Florez. Suellen Aparecida Alves provided data analysis. Patricia Los Weinert provided statistical analysis. Supervision was performed by Elaine Regina Lopes Tiburtius. All authors have read and approved the final manuscript.

References and Notes

- [1] Rehan, M.; Sharkawy, A.; El Fadly, G. *J. Crop. Res. Fert.* **2016**, *1*, 1. [\[Crossref\]](#)
- [2] Solomon, J.; Kumar, A.; Satheja, V. *Biomed. Biotechnol.* **2013**, *14*, 1162. [\[Crossref\]](#)
- [3] Kosmky, A.; Roth, Z. *Reprod. Toxicol.* **2016**, *67*, 15. [\[Crossref\]](#)
- [4] Hayes, B.; Beasley, L.; Solla, S.; Iguchi, T.; Ingraham, H.; Kestemont, P.; Kniewald, J.; Kniewald, Z.; Langlois, V.; Luque, H.; Mccoy, K.; Munoz-De-Toro, M.; Oka, T.; Oliveira, C.; Orton, F.; Ruby, S.; Suzawa, M.; Mendoza, L.; Trudeau, V.; Costa, A.; Willingham, E. *J. Steroid Biochem. Mol. Biol.* **2011**, *127*, 64. [\[Crossref\]](#)
- [5] Bombardi, L. *Geografia do Uso de Agrotóxicos no Brasil e Conexões com a União Europeia*, 1th ed. São Paulo: FFLCH - USP, 2017.
- [6] Hildebrandt, A.; Guillamon, M.; Lacorte, S.; Tauler, R.; Barcelo, D. *Water Res.* **2008**, *42*, 3315. [\[Crossref\]](#)
- [7] Solomon K. R.; Giesy J.P.; Lapoint T. W.; Giddings J. M.; Richards R. P. *Environ. Toxicol. Chem.* **2013**, *32*, 10. [\[Crossref\]](#)
- [8] Rinsky J. L.; Hopenhayn C.; Golla V.; Browning S.; Bush H. M. *Public Health Rep.* **2012**, *127*, 72. [\[Crossref\]](#)
- [9] Pinter, A.; Torok, G.; Borszonyi, M.; Surjan, A.; Csik, M.; Klecseny, Z.; Kocsis, Z. *Neoplasma* **1990**, *37*, 533. [\[Crossref\]](#)

- [10] Pathak, R. K.; Dikshit, A. K. *Int. J. Ecosyst.* **2011**, *1*, 14. [\[Crossref\]](#)
- [11] Balci, B.; Oturan, N.; Cherrier, R.; Oturana, M. *Water Res.* **2009**, *43*, 1924. [\[Crossref\]](#)
- [12] Reilly, T.; Smalling, K.; Orlando, J.; Kuivila, K. *Chemosphere* **2012**, *89*, 228. [\[Crossref\]](#)
- [13] Sass, B.; Colangelo, A. *J. Occup. Environ. Health* **2006**, *12*, 260. [\[Crossref\]](#)
- [14] Vonberg, D.; Vanderborght, J.; Cremer, N.; Putz, T.; Herbst, M.; Vereecken, H. *Water Res.* **2014**, *50*, 294. [\[Crossref\]](#)
- [15] Available from: DPR, department of pesticide regulation, https://www.cdpr.ca.gov/docs/emon/grndwtr/atrazin_e.htm. Access October, 2019.
- [16] Acero, J.; Stemmler, K.; Von Gunten, U. *Environ. Sci. Technol.* **2000**, *34*, 591. [\[Crossref\]](#)
- [17] Ormad, M. P.; Miguel, N.; Claver, A.; Matesanz, J. M.; Ovelleiro, J. L. *Chemosphere* **2008**, *71*, 97. [\[Crossref\]](#)
- [18] Carboneras, B.; Villasenor, J.; Fernandez-Morales, F. J. *Bioresour. Technol.* **2017**, *243*, 1044. [\[Crossref\]](#)
- [19] Jiménez, M.; Oller, I.; Maldonado, I.; Malato, S.; Hernández-Ramírez A.; Zapata, A.; Peralta-Hernández, J. *Catal. Today* **2011**, *161*, 214. [\[Crossref\]](#)
- [20] Saltmiras, D.; Lemley, A. *Water Res.* **2002**, *36*, 5113. [\[Crossref\]](#)
- [21] Chan, K.; Chu, W. *Chemosphere* **2003**, *51*, 305. [\[Crossref\]](#)
- [22] Nelieu, S.; Kerhoas, L.; Einhorn, J. *Environ. Sci. Technol.* **2000**, *34*, 430. [\[Crossref\]](#)
- [23] Cheng, M.; Zeng, G.; Huang, D.; Lai, C.; Xu, P.; Zhang, C.; Liu, Y.; Wan, J.; Gong, X.; Zhu, Y. *J. Hazard. Mater.* **2016**, *312*, 184. [\[Crossref\]](#)
- [24] Bokare, A.; Choi, W. *J. Hazard. Mater.* **2014**, *275*, 121. [\[Crossref\]](#)
- [25] Wang, N.; Zheng, T.; Zhang, G.; Wang, P. *J. Environ. Chem. Eng.* **2016**, *4*, 762. [\[Crossref\]](#)
- [26] Tayade, R.; Natarajan, T.; Bajaj, H. *Ind. Eng. Chem. Res.* **2009**, *48*, 10262. [\[Crossref\]](#)
- [27] Ghosh, P.; Achari, G.; Langford, H. *J. Phys. Chem.* **2008**, *112*, 10310. [\[Crossref\]](#)
- [28] Matafonova, G.; Batoev, V. *Water Res.* **2018**, *132*, 177. [\[Crossref\]](#)
- [29] Farre, M.; Franch, M.; Malato, S.; Ayllon, J.; Peral, J.; Domenech, X. *Chemosphere* **2005**, *58*, 1127. [\[Crossref\]](#)
- [30] Borrás, N.; Oliver, R.; Arias, C.; Brillas, E. *J. Phys. Chem.* **2010**, *114*, 6613. [\[Crossref\]](#)
- [31] Chu, W.; Chan, K.; Kwan, C.; Choi, K. *Chemosphere* **2007**, *67*, 755. [\[Crossref\]](#)
- [32] Pignatello, J.; Oliveros, E.; Mackay, A. *Crit. Rev. Environ. Sci. Technol.* **2006**, *36*, 84. [\[Crossref\]](#)
- [33] Khan, J.; He, X.; Khan, H.; Shah, N.; Dionysiou, D. *Chem. Engin. J.* **2013**, *218*, 376. [\[Crossref\]](#)
- [34] Du, Y.; Zhao, L.; Su, Y. *J. Hazard. Mater.* **2011**, *195*, 291. [\[Crossref\]](#)
- [35] Carra, I.; Sánchez, J.; Malato, S.; Autin, O.; Jefferson, B.; Jarvis, P. *Chem. Eng. J.* **2015**, *264*, 690. [\[Crossref\]](#)
- [36] Davididou, K.; Monteagudo, J.; Chatzisyneon, E.; Durán, A.; Expósito, A. *Sep. Purif. Technol.* **2017**, *172*, 227. [\[Crossref\]](#)
- [37] Moreira, N.; Sousa, J.; Macedo, G.; Ribeiro, A.; Barreiros, L.; Pedrosa, M.; Faria, J.; Pereira, F.; Silva, F.; Segundo, M.; Manaia, C.; Nunes, O.; Silva, A. *Water Res.* **2016**, *94*, 10. [\[Crossref\]](#)
- [38] Liwei, C.; Xiaoxin, H.; Ying, Y.; Canlan, J.; Cheng, B.; Chao, L.; Miao Yue, Z.; Tianming, C. *Chem. Eng. J.* **2018**, *351*, 523. [\[Crossref\]](#)
- [39] Benzaquena, T.; Cuello, N.; Alfano, O.; Eimer, G. *Catal. Today* **2017**, *296*, 51. [\[Crossref\]](#)
- [40] Kassinos, D.; Varnava, N.; Michael, C.; Piera, P. *Chemosphere* **2009**, *74*, 866. [\[Crossref\]](#)
- [41] Zhanqi, G.; Shaogui, Y.; Na, T.; Cheng, S. *J. Hazard. Mater.* **2007**, *145*, 424. [\[Crossref\]](#)
- [42] Farre, M. J.; Franch, M. I.; Malato, S.; Ayllon, J. A.; Peral, J.; Domenech, X. *Chemosphere* **2005**, *58*, 1127. [\[Crossref\]](#)
- [43] Badawy, M. I.; Ghaly, M. Y.; Gad-Allah, T. A. *Desalination* **2006**, *194*, 166. [\[Crossref\]](#)
- [44] Balci, B.; Oturan, N.; Cherrier, R.; Oturan, A. M. *Water Res.* **2009**, *43*, 924. [\[Crossref\]](#)
- [45] Malpass, G.; Miwa, D.; Machado, S.; Olivi, P.; Motheo, A. *J. Hazard. Mater.* **2006**, *137*, 565. [\[Crossref\]](#)
- [46] McMurray, T.; Dunlop, P.; Byrne, J. *J. Photochem. Photobiol. A: Chem.* **2006**, *182*, 43. [\[Crossref\]](#)
- [47] Zazo, J.; Casas, J.; Mohedano, A.; Rodriguez, J. *Water Res.* **2009**, *43*, 4063. [\[Crossref\]](#)
- [48] Monteagudo, J.; Durán, A.; San Martín, I.; Aguirre, M. *Appl. Catal. B: Environ.* **2009**, *89*, 510. [\[Crossref\]](#)
- [49] Chen, J.; Loeb, S.; Hong Kim, J. *Water Res. Technol.* **2017**, *3*, 188. [\[Crossref\]](#)
- [50] Rasoulifard, M.; Fazli, M.; Eskandarian, M. *J. Ind. Eng. Chem.* **2015**, *24*, 121. [\[Crossref\]](#)
- [51] Daneshvar, N.; Aleboyyeh, A.; Khataee, A. *Chemosphere* **2005**, *59*, 761. [\[Crossref\]](#)
- [52] Andreozzi, R.; Caprio, V.; Insola, A.; Marotta, R. *Catal. Today* **1999**, *53*, 51. [\[Crossref\]](#)
- [53] Zoschke, K.; Dietrich, N.; Bornick, H.; Worch, E. *Water Res.* **2012**, *46*, 5365. [\[Crossref\]](#)
- [54] Komtchou, S.; Dirany, A.; Drogui, P.; Robert, D.; Lafrance, P. *Water Res.* **2017**, *125*, 91. [\[Crossref\]](#)
- [55] Wardenier, N.; Vanraes, P.; Nikiforov, A.; Van Hulle, S.; Leys, C. *J. Hazard. Mater.* **2019**, *362*, 238. [\[Crossref\]](#)
- [56] Luo, C.; Ma, J.; Jiang, J.; Liu, Y.; Song, Y.; Yang, Y.; Guan, Y.; Wu, D. *Water Res.* **2015**, *80*, 99. [\[Crossref\]](#)
- [57] Horrobin S. *J. Chem. Soc.* **1963**, *1*, 4130. [\[Crossref\]](#)
- [58] Jacomini, A.; Bonato, S.; Eustáquio, W. *J. Liq. Chromatogr. Relat. Technol.* **2003**, *26*, 1885. [\[Crossref\]](#)
- [59] Oliveira, M.; Nogueira, R.; Neto, J.; Jardim W.; Rohwedder, J. *Quim. Nova*, **2001**, *24*, 188. [\[Crossref\]](#)
- [60] Available from: Standard Methods, Total Organic Carbon Analyzer: 5310C, 2017. https://www.nemi.gov/methods/method_summary/5718/. Access October, 2019.
- [61] Goldstein, S.; Rabani, J. *Environ Sci Technol.* **2008**, *42*, 3248. [\[Crossref\]](#)
- [62] Rodríguez, C.; Fernandes, J.; Tavares, P.; Marco, S.; Peres, A. *Chemosphere* **2016**, *145*, 351. [\[Crossref\]](#)
- [63] Shie, Je.; Lee, C.; Chiou, C.; Changa, C.; Chang, C.; Chang, C. *J. Hazard. Mater.* **2008**, *155*, 164. [\[Crossref\]](#)

- [64] Lutze, H.; Kerlin, N.; Schmidt, T. *Water Res.* **2015**, 72, 349. [\[Crossref\]](#)
- [65] Khan, J.; He, X.; Shah, N.; Khan, H.; Hapeshi, E.; Kassinos, D.; Dionysiou, D. *Chem. Eng. J.* **2014**, 252, 393. [\[Crossref\]](#)
- [66] Pouran, S.; Aziz, A.; Wan, W. *J. Ind. Eng. Chem.* **2015**, 21, 53. [\[Crossref\]](#)

How to cite this article

Florez, P. L. S.; Alves, S. a.; Weinert, P. L.; Tiburtius, E. R. L. *Orbital: Electron. J. Chem.* **2021**, 13, 160. DOI: <http://dx.doi.org/10.17807/orbital.v13i2.1531>